Supporting Online Material for

Dynamic Visualization of Thrombopoiesis Within Bone Marrow

Tobias Junt, Harald Schulze, Zhao Chen, Steffen Massberg, Tobias Goerge, Andreas Krueger, Denisa D. Wagner, Thomas Graf, Joseph E. Italiano Jr., Ramesh A. Shivdasani,* Ulrich H. von Andrian*

*To whom correspondence should be addressed.
E-mail: uva@hms.harvard.edu (U.H.v.A.);
ramesh_shivdasani@dfci.harvard.edu (R.A.S.)

Published 21 September 2007, *Science* **317**, 1767 (2007)

DOI: 10.1126/science.1146304

This PDF file includes:

Materials and Methods
Figs. S1 to S4
References

Other Supporting Online Material for this manuscript includes the following:
(available at www.sciencemag.org/cgi/content/full/317/5845/1767/DC1)

Movies S1 to S11

Supporting Online Material

Materials and Methods

Mice.

CD41-EYFP$^{ki/+}$ mice (S*1*) and wild-type controls were bred and housed under specific pathogen-free conditions. All experiments were done according to National Institute of Health guidelines and were approved by Institutional Animal Care and Use Committees at Harvard Medical School, the Center for Blood Research Institute, and Dana-Farber Cancer Institute.

Isolation and activation of platelets.

All antibodies and fluorescent streptavidin conjugates were purchased from BD Biosciences, unless otherwise mentioned. Particular care was taken to avoid chilled reagents or equipment. All centrifugations were performed in the presence of 2 μg/ml prostacyclin (PGI_2) or in Tyrodes buffer (TB; 8 g/l NaCl, 1.015 g/l $NaHCO_3$, 0.195 g/l KCl, 1 g/l bovine serum albumin, 1 g/l glucose, pH6.5). All antibody stainings were performed at room temperature. Platelets were resuspended in TB (pH 6.5) for centrifugation, and in TB (pH 7.4) for platelet activation or staining.

For analysis of platelets, blood from the retro-orbital sinus was collected into TB containing 30 U/ml heparin (American Pharmaceutical Partners, Los Angeles, CA) or by

cardiac puncture with heparinized syringes from anesthetized mice (5mg/ml Ketamine, 1mg/ml Xylazine in saline) into heparin. Platelet-rich plasma (PRP) was collected by removal of corpuscular blood constituents at 300 *g*, and platelets were washed twice in TB (pH 6.5) at 1200 *g*. After resuspension in TB (pH 7.4), cells were stained at room temperature and collected on a FACScalibur or a FACScan (BD Biosciences) flow cytometer with Cellquest software. Platelets were activated by the addition of 1 mM PAR4 peptide (GYPGKF, Advanced ChemTech, Louisville, KY) in TB containing 1 mM $CaCl_2$ and 1 mM $MgCl_2$. Platelet activation was monitored by flow cytometry with anti-CD62P-PE (Emfret Analytics, Würzburg, Germany). Alternatively, aggregation was monitored at a density of 5-10 x 10^7 platelets/ml by light transmission with a Chrono-Log aggregometer (Havertown, PA), and analyzed with Aggrolink software (Chrono-Log). Platelets were enumerated relative to Fluoresbrite beads (BD Pharmingen), after co-stain for CD41 (MWReg30, BD Pharmingen). Total platelet numbers per mouse were extrapolated from these measurements assuming a total blood volume of 2 ml per mouse.

Isolation and analysis of proplatelets.

Mice were anesthetized by intraperitoneal injection of 2.5% (Tribromoethanol, Fluka, Buchs, Switzerland) in saline and exsanguinated retro-orbitally with heparinized capillary tubes. Platelet-rich plasma (PRP) was isolated by centrifugation and fixed by 1:1 dilution with 8% paraformaldehyde in Hanks' Balanced Salt Solution (HBSS) for 20 min. 5 μl of fixed PRP were placed in wells of a 24-well plate each containing a poly-L-lysine coated

coverslip. The plate was centrifuged at 1500 g for 5 min. Adherent cells were washed extensively with phosphate-buffered saline (PBS), permeabilized with 0.5% Triton X-100 in HBSS for 3 min, and washed again with PBS. After overnight treatment with blocking buffer (10% FCS in PBS), anti-β1-tubulin antibody (gift from Nick Cowan, New York University Medical Center, NY) was added at 1:1000 in blocking buffer for 1 h at room temperature. After extensive washing with PBS, 2 μg/ml AlexaFluor 488-labeled goat-anti-rabbit antibody (Molecular Probes, Eugene, OR) in PBS was added for 1h. Coverslips were washed, and mounted on slides with aqua poly/mount (Polysciences, Warrington, PA). Images were acquired on a Zeiss Axiovert 200 microscope with a 100X objective (NA 1.4) and 100W mercury lamp equipped with an OrcaIIER CCD camera under the control of Metamorph software, and processed with Adobe Photoshop software.

Isolation and analysis of bone marrow megakaryocytes.

Care was taken to avoid chilled reagents or equipment. Bone marrow was flushed from femurs of mice with ACD/PBS working solution (5 parts PBS, 2% BSA, 1 part ACD buffer (2.2% sodium citrate, 0.8% citric acid, 2.2% glucose in water), 3 μM prostaglandin E1). Bone marrow suspensions were filtered through a 100 μm cell strainer and MKs were pelleted at 80 g for 10 min. After washing in ACD/PBS at 300 g and resuspension in ACD/PBS, 2 μg/ml Fc-block (2.4G2, BD Pharmingen) were added for 10 min under constant gentle agitation. Subsequently, anti-CD61-PE (BD Pharmingen) and anti-CD41

were added at 2 μg/ml for 20 min. Suspensions were washed and resuspended in 1ml ACD/PBS. 40 μl of pre-washed anti-rat M-450 beads (Dynal Invitrogen, Carlsbad, CA) were added for 20 min under gentle agitation. CD41+ cells were magnetically selected and resuspended in ACD/PBS containing 0.025% Triton X-100 and 8 μg/ml 7-AAD (BD Pharmingen), and analyzed with a FACScan within 30 min after staining.

Alternatively, bone marrow from femurs of CD41-EYFP$^{ki/+}$ mice was centrifuged at 300 *g* on glass slides, Cells were formaldehyde-fixed and permeabilized with 0.5% Triton X-100 in PBS prior to staining with 10 μg/ml of anti-CD61-biotin and streptavidin-Cy2 (Jackson ImmunoResearch Laboratories, West Grove, PA), followed by a 3 min incubation with 5 mg/ml 4',6-Diamidino-2-phenylindol (DAPI). Cytospins were embedded in FluorSave Reagent (Calbiochem, San Diego, CA), imaged on an Olympus IX70 inverted fluourescence deconvolution microscope using a 40x/1.35 NA air objective lens for MKs. Images were analyzed with a CM350 CCM camera (Applied Precision, Issaquah, WA). Images were analyzed with DeltaVision software (Applied Precision) and Adobe Photoshop (Adobe Systems, San Diego, CA).

Total numbers of bone marrow MKs was estimated based on the work by Long and Boggs (S*2, S3*)

In vitro culture of MKs under shear conditions.

MKs were prepared and transduced with an EGFP-expressing retrovirus as described (S*4*). 2x10^5 MKs from day 3 cultures were cultured in triplicates on top of 5 μm

transwells. After two hours, plates were agitated in an environmental shaker at 50 rpm or rested for three hours. One hour later, contents of the lower well were quantified by flow cytometry, gating on $EGFP^+$ events, and documented by fluorescence microscopy. Live cells were imaged using a Nikon Eclipse TE300 inverted fluorescent microscope with attached Spot camera (Diagnostic Instruments, Sterling Heights, MI).

Two-photon intravital microscopy of the bone marrow.

Preparation of mouse calvarial bone marrow for intravital imaging was described previously (S*5,* S*6*). Bone marrow vasculature was visualized by injection of fluorescein isothiocyanate-dextran (2 MDa, Sigma) immediately before imaging. Images were acquired with an Olympus RX50WI fluorescence microscope equipped with a 20X objective with a numerical aperture of 0.95, and a Radiance 2100MP Multiphoton microscopy system, controlled by Lasersharp software (BioRad). A tunable MaiTai broad-band Ti:S laser (Spectra Physics) was used at 900 nm to capture EYFP and FITC-dextran fluorescence (515/30, 550/30 filters, and 450/80 for second harmonic signal of the bone). Stacks of x-y sections were acquired every 7-15 s, at a distance of 0.5-4 μm in z through a three-channel detector: Four-dimensional acquisition parameters for each movie are specified in the Legends to Supporting Movies. Volocity Software (Improvision) was used to generate movies, to measure volumes and distances, and to track mobile MK fragments semi-automatically. Where necessary, the data sets were corrected for tissue drift by the StackReg plugin in ImageJ (Rasband, NIH, Bethesda,

Maryland, USA, http://rsb.info.nih.gov/ij/, 1997-2006.). Motility parameters were calculated from centroid coordinates by a customized program in Matlab (MathWorks), as previously described (S7). To analyze volumes of MKs or MK fragments, $EYFP^+$ areas were selected on subsequent optical sections with Photoshop, and automatically reassembled and measured in Volocity. Some mice were treated for 2.5 days before imaging with 1 ng/g body weight PEGylated TPO (Amgen, Thousand Oaks, CA) or recombinant mouse TPO (R&D systems, Minneapolis, MN) i.p.

3D Reconstruction and analysis of MKs in BM of living mice.

For 3D reconstruction of MKs, EYFP-positive areas from intravital 3D renderings were selected in Photoshop, then stacked together in Volocity, with the parameters used for recording. Volumes and surface areas were calculated automatically, maximal diameters were measured manually. Wadell sphericity is a measure for roundness and defined as the ratio of the surface area of a sphere with the same volume as the given MK (V_{MK}) to the surface area (A_{MK}) of that given MK. A perfectly spherical entity has a Wadell sphericity index of 1. It was calculated as:

$$\psi = \frac{\sqrt[3]{\pi(6V_{MK})^2}}{A_{MK}}$$

Fig. S1

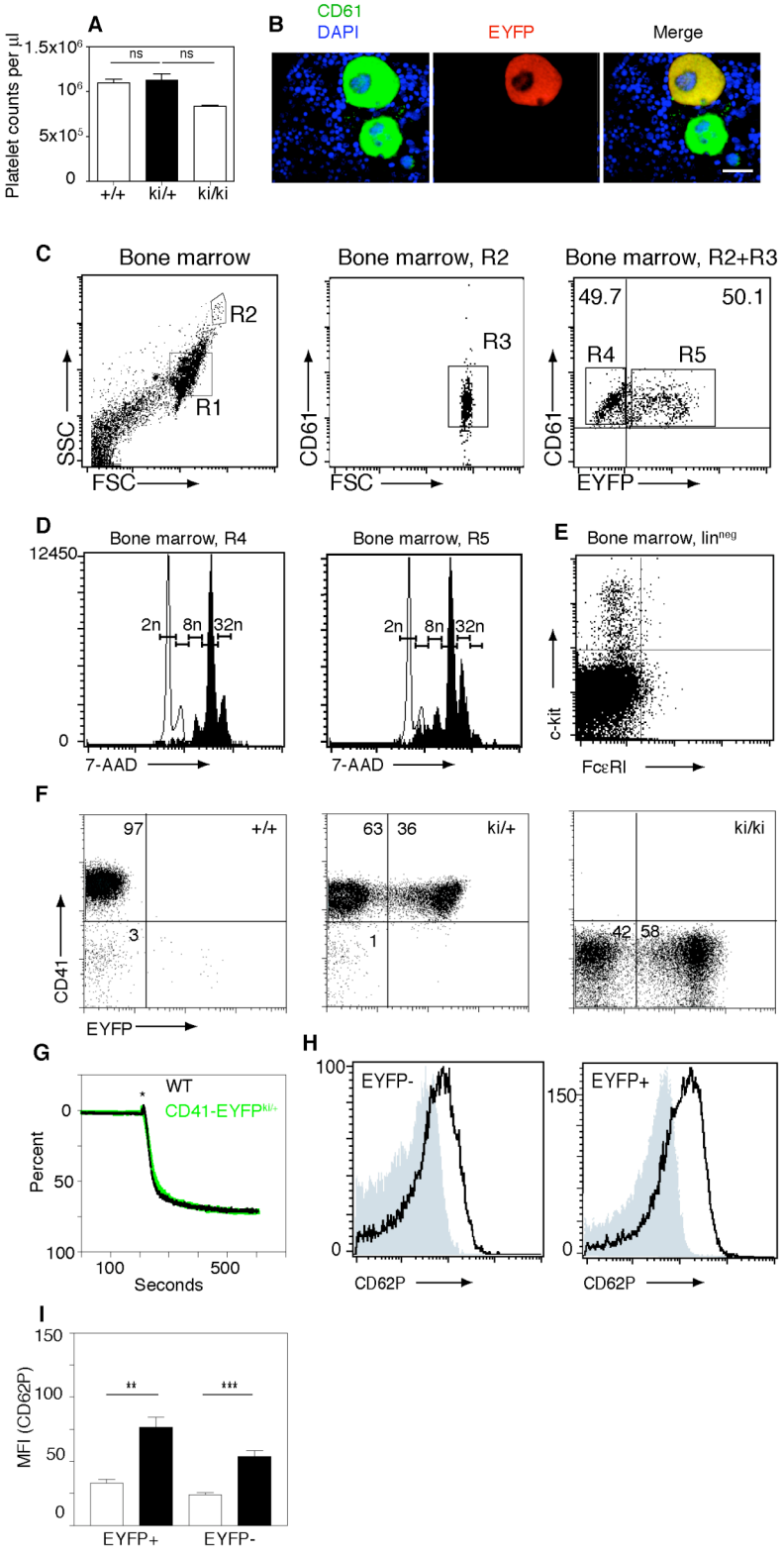
A
Platelet counts per µl
1.5x10⁶
10⁶
5x10⁵
0
ns
ns
+/+
ki/+
ki/ki
B
CD61
DAPI
EYFP
Merge
C
Bone marrow
R2
R1
SSC
FSC
Bone marrow, R2
R3
CD61
FSC
Bone marrow, R2+R3
49.7
50.1
R4
R5
CD61
EYFP
D
Bone marrow, R4
12450
2n
8n
32n
0
7-AAD
Bone marrow, R5
2n
8n
32n
7-AAD
E
Bone marrow, lin^neg
c-kit
FcεRI
F
97
+/+
3
CD41
EYFP
63
36
ki/+
1
ki/ki
42
58
G
WT
CD41-EYFP^ki/+
Percent
0
50
100
100
500
Seconds
H
EYFP-
100
0
CD62P
EYFP+
150
0
CD62P
I
MFI (CD62P)
150
100
50
0
**
***
EYFP+
EYFP-

Figure S1 (see previous page): Characterization of BM-resident MKs and peripheral blood platelets in CD41-EYFP^{ki} mice.
Experiments were done in mice that had not been treated with TPO. **(A)** Total platelet count in peripheral blood of WT, CD41-EYFP$^{ki/+}$ and CD41-EYFP$^{ki/ki}$ mice. While CD41-EYFP$^{ki/+}$ mice show no platelet abnormalities, *CD41-EYFP$^{ki/ki}$* mice showed reduced platelet counts, likely owing to impaired MK differentiation in the absence of CD41 (S*8*). Data were analyzed using one-way ANOVA with Bonferroni post-test. **(B)** Cytospin preparation of BM from non-TPO treated CD41-EYFP$^{ki/+}$ mice, counterstained with anti-CD61 and DAPI. Although all *CD41* loci are presumed to be transcriptionally active in polyploid MKs (S*9*), there were also EYFP$^-$ MKs in *CD41-EYFP$^{ki/+}$* mice, which can be attributed to epigenetic silencing (S*1*). Scale bar corresponds to 40 μm. **(C)** Frequency of EYFP$^+$ MKs in BM of non-TPO treated CD41-EYFP$^{ki/+}$ mice. Left panel: CD41$^+$ enriched BM cells showing gate settings for small leukocytes (R1) and large mononuclear cells (R2); middle panel: CD61 expression on large cells (R2) identifies MKs (combined gates R2 and R3); right panel: heterogeneous EYFP expression by MKs. Results are representative of 3 independent experiments, mean frequency of EYFP$^+$ MKs: 46.2% (34-64%). **(D)** MKs are polyploid by 7-AAD staining. Left panel: EYFP$^-$ MKs (defined by combined gates R2, R3 and R4 shown in (B)); right panel: EYFP$^+$ MKs (combined gates R2, R3 and R5). Ploidy analysis of lymphocytes/granulocytes (gate R1) is shown for comparison (empty histograms), level of ploidy is denoted. Results are representative of 3 independent experiments. **(E)** Staining of mouse BM for FcεR1 and c-kit fails to detect double-positive cells, indicating that normal BM does not contain mature mast cells, which are the only other nucleated cells besides MKs that are known to express CD41 (S*10*). The dot plot was acquired after gating on cells negative for CD3, CD4, CD8, B220, Gr-1, CD11b, CD11c and NK1.1. Results are representative of 2 separate experiments. **(F)** EYFP and CD41/CD61 heterodimer expression on platelets of WT (+/+), CD41-EYFP$^{ki/+}$ and CD41-EYFP$^{ki/ki}$ mice. Peripheral blood platelets were stained with anti-CD41. One representative of n=2-6 individuals per group is shown, mean frequency of EYFP$^+$ platelets in CD41-EYFP$^{ki/+}$ mice: 48.4%. **(G)** Aggregation kinetics of platelets from WT (black line) and CD41-EYFP$^{ki/+}$ (green line) mice upon stimulation with PAR4 pepetide. The moment of addition of PAR4 peptide is denoted with an asterisk. Results are representative of 4 independent experiments. **(H)** CD62P surface expression on EYFP$^-$ (left panel) and EYFP$^+$ (right panel) platelets from CD41-EYFP$^{ki/+}$ mice prior to (grey histograms) and following activation with 2 μM PAR4 peptide (solid line histogram). One representative measurement of four independent experiments is shown. **(I)** Mean fluorescence intensity (MFI) of CD62P expression; ** $p<0.01$, *** $p<0.001$ unpaired student's t-test.

Fig. S2

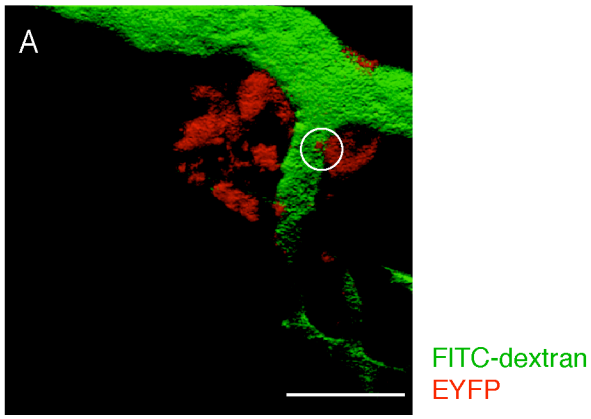

Figure S2: Visualization of MK differentiation in CD41-EYFP$^{ki/+}$ control mice that were not treated with TPO.
Perivascular MKs with large proplatelet extensions, including protrusions into adjacent blood vessels (white circle). Scale bar corresponds to 50 μm.

Fig. S3

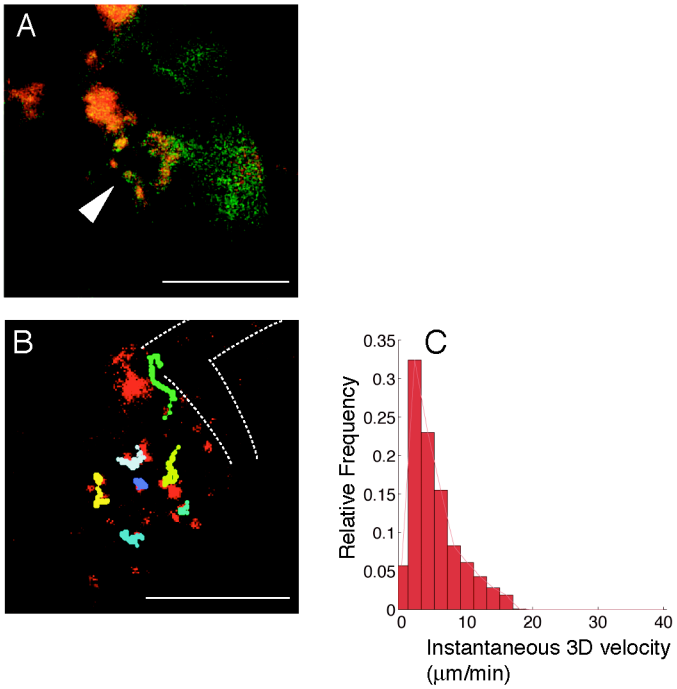

Figure S3: Formation and motility of interstitial proplatelets. (A) Perivascular megakaryocyte, proplatelets (arrowhead) that appear as beads-on-a-string. Size bar corresponds to 25 μm. **(B)** Same area as in (A) 3 h later, red channel only. Approximate locations of blood vessels are indicated by dashed lines, some tracks of $EYFP^+$ MK fragments over 30 min are exemplified in color. Size bar corresponds to 50 μm. **(C)** Instantaneous 3D velocity of MK fragments, based on the analysis of one representative of n=4 movies.

Fig. S4

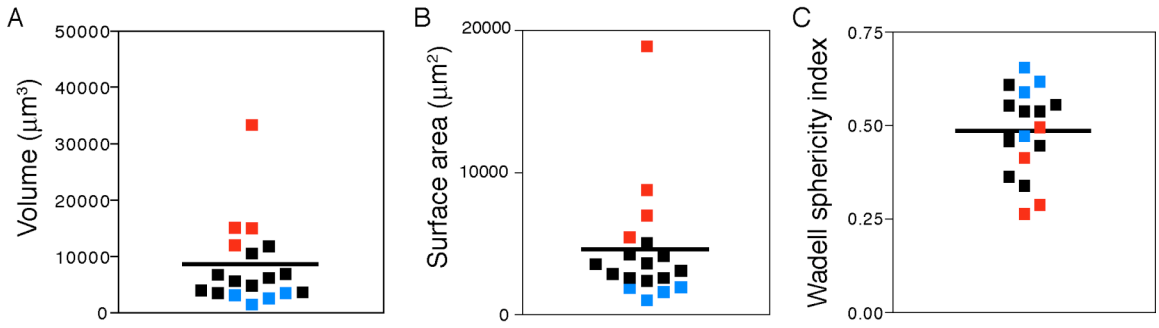

Figure S4: Size and shape parameters of MKs in CD41-EYFP$^{ki/+}$ control mice that were not treated with TPO.
(A) MK volume, **(B)** surface area, and **(C)** Wadell's sphericity index in nontreated CD41-EYFP$^{ki/+}$ mice. Data points highlighted in red are MKs with highest volumes, data points highlighted in blue are MKs with lowest volumes. Note that high volumes correlate with high surface areas and low sphericities (red squares), and low volumes with low surface areas and high sphericities (blue squares). This shows that the process of MK differentiation is not qualitatively different from TPO-treated mice (compare Fig. 3D-F). However, the inverse correlation of MK volume and sphericity did not apply strictly to all cells (data not shown), which suggests that MK size and shape may be regulated independently.

Legends to Supporting Online Movies

Movie S1:

EYFP+ MKs (red) localize close to BM sinusoids in TPO-treated mice. The blood stream is counterstained with FITC-dextran (green).

Image represents a stack of 27 sections (z step of 2 μm), averaged over three frames and a pixel density of 512x512. Rotation +/- 20° from the vertical plane of view. Scale bar corresponds to 50 μm.

Movie S2:

MKs in the BM of TPO-nontreated mice.

Movie represents a stack of 36 sections (z step of 1 μm) at a pixel density of 512x512. At the beginning and the end of the movie, a 3D reconstruction of the field of view is shown. White circle represents intravascular MK protrusion. Scale bar corresponds to 50 μm.

Movie S3:

Irregular shaped MK (red) with presumed proplatelets in the proximity of BM sinusoids, counterstained with FITC-dextran (green).

Image respresents a stack of 27 sections (z step of 2 μm) at a pixel density of 1024x1024. Rotation +/- 20° from the vertical plane of view. Scale bar corresponds to 50 μm.

Movie S4:

MK with an array of fragments nearby (red) in the proximity of BM sinusoids, counterstained with FITC-dextran (green). The fragments may be connected by a filament that is below the resolution of the MP-IVM.

Image represents a stack of 32 sections (z step of 2 μm) at a pixel density of 1024x1024. Rotation +/- 20° from the vertical plane of view. Size bar corresponds to 50 μm.

Movie S5:

Cytoplasmic protrusions from an EYFP+ MK form proplatelets and intermediate swellings.

Three movies of the same z-stack (21 sections, z step of 0.5 μm), pasted together. Pixel density of 512x512, over a total of 90 frames, with a frame rate of 15 s. White numbers in upper right corner are minutes and seconds, scale bar corresponds to 50 μm.

Movie S6:

Movement of proplatelets, intermediate swellings and MK progeny in the interstitium, close to the MK. Blood stream is counterstained with FITC-dextran (green).

Z-stack of 12 sections (z step of 2 μm) at a pixel density of 256x256 over 200 frames, at a frame rate of 7 s. White numbers in upper left corner are minutes and seconds, scale bar corresponds to 50 μm. Second harmonic signal of the bone is visible in blue.

Movie S7:

Elaborate proplatelets extend into the lumen of a BM sinusoid vessel.

Scan of 31 sections (z step of 2 μm), at a pixel density of 512x512, averaged over three frames. White numbers in the upper right corner are depth in micrometers, scale bar corresponds to 50 μm.

Movie S8:

Formation of a pseudopodium by a EYFP+ MK (red) into a BM sinusoid. The blood stream is counterstained with FITC-dextran (green), and second harmonic emission signal of the collagen appears in blue.

Z-stack of 12 sections (z step of 4 μm) at a pixel density of 256x256, over 61 frames, with a frame rate of 15 s. White numbers in the upper left corner are minutes and seconds, scale bar corresponds to 50 μm. Arrowhead shows formation of MK pseudopodium at the sinusoid vessel.

Movie S9:

Large EYFP+ fragment, potentially a whole MK (red) is shed into a BM sinusoid. It partially occludes the blood flow upstream. Blood stream is counterstained with FITC-dextran (green).

Six movies of the same z-stack (11 sections, z step of 4 μm) pasted together. Pixel density of 256x256, over a total of 735 frames, with a frame rate of 15 s. White numbers in upper left corner are hours, minutes and seconds, scale bar corresponds to 50 μm.

Movie S10:

Slow shedding of EYFP+ MK fragment (red, arrowhead) into a BM sinusoid. Blood stream is counterstained with FITC-dextran (green).

Z-stack of 14 sections (z step of 4 μm) at a pixel density of 256x256, over 161 frames, with a frame rate of 15 s. White numbers in upper left corner are minutes and seconds, scale bar corresponds to 50 μm. White arrowhead shows proplatelet shed into the circulation.

Movie S11:

Rapid shedding of EYFP+ MK fragment (red, arrowhead) in a BM sinusoid by the force of the blood stream. Blood stream is counterstained with FITC-dextran (green).

Z-stack of 14 sections (z step of 4 μm) at a pixel density of 256x256, over 161 frames, with a frame rate of 15 s. White numbers in upper left corner are minutes and seconds, scale bar corresponds to 50 μm. White arrowhead shows proplatelet shed into the circulation.

Supporting References

S1. J. Zhang *et al.*, *Exp Hematol* **35**, 490 (2007).
S2. M. W. Long, N. Williams, *Leuk Res* **6**, 721 (1982).
S3. D. R. Boggs, *Am J Hematol* **16**, 277 (1984).
S4. Z. Chen *et al.*, *Blood* (Mar 28, 2007).
S5. I. B. Mazo *et al.*, *J Exp Med* **188**, 465 (1998).
S6. C. Sumen, T. R. Mempel, I. B. Mazo, U. H. von Andrian, *Immunity* **21**, 315 (2004).
S7. T. R. Mempel, S. E. Henrickson, U. H. Von Andrian, *Nature* **427**, 154 (2004).
S8. M. K. Larson, S. P. Watson, *Blood* **108**, 1509 (2006).
S9. H. Raslova *et al.*, *Blood* **101**, 541 (2003).
S10. T. Oki *et al.*, *J Immunol* **176**, 52 (2006).